Research Article | Vol. 7, No. 1 | 1 Jan 2017 | OPTICAL MATERIALS EXPRESS 170

Optical Materials EXPRESS

Spectroscopy and CW first laser operation of Yb-doped $Gd_3(Al_{0.5}Ga_{0.5})_5O_{12}$ crystal

GUIDO TOCI,[1] ANGELA PIRRI,[2,*] WITOLD RYBA-ROMANOWSKI,[3] MAREK BERKOWSKI,[4] AND MATTEO VANNINI[1]

[1]*C.N.R. - National Research Council, Istituto Nazionale di Ottica, INO-CNR, Via Madonna del Piano 10, I-50019 Sesto Fiorentino (FI), Italy*
[2]*C.N.R. - National Research Council, Istituto di Fisica Applicata "Nello Carrara," IFAC-CNR, Via Madonna del Piano 10, I-50019 Sesto Fiorentino (FI), Italy*
[3]*Institute of Low Temperature and Structure Research, Polish Academy of Sciences, Okólna 2, 50-422 Wroclaw, Poland*
[4]*Institute of Physics, Polish Academy of Sciences, Aleja Lotników 32/46, 02-668 Warsaw, Poland*
**a.pirri@ifac.cnr.it*

Abstract: We present the spectroscopic characterization and laser operation of a 2%*at.* Yb doped $Gd_3(Al_{0.5}Ga_{0.5})_5O_{12}$ (Yb:GAGG) crystal, grown with the Czochralski method. We determined the absorption and the emission spectrum, the upper level lifetime, and the thermal conductivity. The internal disordered structure determines a significant broadening of the emission band (12.1 nm FWHM) with respect to the parent composition Yb:GGG (8 nm FWHM). The laser performances were evaluated on an end pumped cavity, using a CW semiconductor laser as the pump source. We obtained a maximum slope efficiency of 60.8% and an optical to optical efficiency of 46.0%, with a maximum output power of 4 W, limited only by the available pump power. The tuning range extends from 995 nm to 1050 nm. To our knowledge this is the first spectroscopic investigation and the first assessment of the laser performance of an Yb:GAGG crystal with this composition (*i.e.* Al/Ga balance = 0.5/0.5).

OCIS codes: (140.3580) Lasers, solid-state; (140.5680); Rare earth and transition metal solid-state lasers; (140.3600) Lasers, tunable; (160.3380) Laser materials.

References and links

1. F. Wang, Z. Qin, G. Xie, P. Yuan, L. Qian, X. Xu, and J. Xu, "8.5 W mode-locked Yb:$Lu_{1.5}Y_{1.5}Al_5O_{12}$ laser with master oscillator power amplifiers," Appl. Opt. **54**(5), 1041–1045 (2015).
2. G. Toci, A. Pirri, J. Li, T. Xie, Y. Pan, V. Babin, A. Beitlerova, M. Nikl, and M. Vannini, "First laser emission of $Yb_{0.15}$:$(Lu_{0.5}Y_{0.5})_3Al_5O_{12}$ ceramics," Opt. Express **24**(9), 9611–9616 (2016).
3. A. Pirri, G. Toci, J. Li, T. Xie, Y. Pan, V. Babin, A. Beitlerova, M. Nikl, and M. Vannini, "Spectroscopic and laser characterization of $Yb_{0.15}$:$(Lu_xY_{1-x})_3Al_5O_{12}$ ceramics with different Lu/Y balance," Opt. Express **24**(16), 17832–17842 (2016).
4. D. W. Luo, C. W. Xu, J. Zhang, X. P. Qin, H. Yang, W. D. Tan, Z. H. Cong, and D. Y. Tang, "Diode pumped and mode-locked Yb:GdYAG ceramic lasers," Laser Phys. Lett. **8**(10), 719–722 (2011).
5. F. Lou, Z. T. Jia, J. L. He, R. W. Zhao, J. Hou, Z. W. Wang, S. D. Liu, B.-T. Zhang, and C. M. Dong, "Efficient High-Peak-Power Wavelength-Switchable Femtosecond Yb:LGGG Laser," IEEE Photonics Technol. Lett. **27**(4), 407–410 (2015).
6. J. Saikawa, Y. Sato, T. Taira, and A. Ikesue, "Absorption, emission spectrum properties, and efficient laser performances of Yb:$Y_3ScAl_4O_{12}$ ceramics," Appl. Phys. Lett. **85**(11), 1898–1900 (2004).
7. M. Tokurakawa, H. Kurokawa, A. Shirakawa, K. Ueda, H. Yagi, T. Yanagitani, and A. A. Kaminskii, "Continuous-wave and mode-locked lasers on the base of partially disordered crystalline Yb^{3+}:$YGd_2[Sc_2](Al_2Ga)O_{12}$ ceramics," Opt. Express **18**(5), 4390–4395 (2010).
8. K. Kamada, T. Yanagida, T. Endo, K. Tsutumi, Y. Usuki, M. Nikl, Y. Fujimoto, A. Fukabori, and A. Yoshikawa, "2inch diameter single crystal growth and scintillation properties of Ce:$Gd_3Al_2Ga_3O_{12}$," J. Cryst. Growth **352**(1), 88–90 (2012).
9. W. Chewpraditkul, P. Bruza, D. Pánek, N. Pattanaboonmee, K. Wantong, W. Chewpraditkul, V. Babin, K. Bartosiewicz, K. Kamada, A. Yoshikawa, and M. Nikl, "Optical and scintillation properties of Ce^{3+} -doped $YGd_2Al_{5-x}Ga_xO_{12}$ (x=2,3,4) single crystal scintillators," J. Lumin. **169**, 43–50 (2016).
10. W. Ryba-Romanowski, J. Komar, T. Niedzwiedzki, M. Glowacki, and M. Berkowski, "Excited state relaxation dynamics and up-conversion phenomena in $Gd_3(Al,Ga)_5O_{12}$ single crystals co-doped with holmium and ytterbium," J. All. Comp. **656**, 573–580 (2016).

#272539 http://dx.doi.org/10.1364/OME.7.000170
Journal © 2017 Received 2 Aug 2016; revised 29 Sep 2016; accepted 4 Oct 2016; published 9 Dec 2016

Optical Materials EXPRESS

11. T. Niedźwiedzki, W. Ryba-Romanowski, J. Komar, M. Głowacki, and M. Berkowski, "Excited state relaxation dynamics and up-conversion phenomena in $Gd_3(Al,Ga)_5O_{12}$ single crystals co-doped with erbium and ytterbium," J. Lumin. **177**, 219–227 (2016).
12. J. Zhang, X. T. Tao, C. M. Dong, Z. T. Jia, H. H. Yu, Y. Z. Zhang, Y. C. Zhi, and M. H. Jiang, "Crystal growth, optical properties, and CW laser operation at 1.06μm of Nd:GAGG crystals," Laser Phys. Lett. **6**(5), 355–358 (2009).
13. A. Agnesi, F. Pirzio, G. Reali, A. Arcangeli, M. Tonelli, Z. Jia, and X. Tao, "Multi-wavelength Nd: GAGG picosecond laser," Opt. Mater. **32**(9), 1130–1133 (2010).
14. B. T. Zhang, J. L. He, Z. T. Jia, Y. B. Li, S. D. Liu, Z. W. Wang, R. H. Wang, X. M. Liu, and X. T. Tao, "Spectroscopy and laser properties of Yb-doped $Gd_3Al_xGa_{5-x}O_{12}$ crystal," Appl. Phys. Express **6**(8), 082702 (2013).
15. F. Lou, L. Cui, Y. B. Li, J. Hou, J. L. He, Z. T. Jia, J. Q. Liu, B. T. Zhang, K. J. Yang, Z. W. Wang, and X. T. Tao, "High-efficiency femtosecond Yb:$Gd_3Al_{0.5}Ga_{4.5}O_{12}$ mode-locked laser based on reduced graphene oxide," Opt. Lett. **38**(20), 4189–4192 (2013).
16. R. Zhao, B. Zhang, Z. Jia, X. Su, F. Lou, H. Zhang, J. He, and F. Liu, "Efficient tri-wavelength actively Q-switched Yb:GAGG laser," Opt. Mater. **39**, 265–268 (2015).
17. Y. Kuwano, S. Saito, and U. Hase, "Crystal growth and optical properties of Nd:GGG," J. Cryst. Growth **92**(1-2), 17–22 (1988).
18. R. A. Young, A. Sakthivel, T. S. Moss, and C. O. Paiva-Santos, "DBWS –9411 – an upgrade of the DBWS *.* programs for Rietveld refinement with PC and mainframe computers," J. Appl. Cryst. **28**(3), 366–367 (1995).
19. H. Kühn, S. T. Fredrich-Thornton, C. Kränkel, R. Peters, and K. Petermann, "Model for the calculation of radiation trapping and description of the pinhole method," Opt. Lett. **32**(13), 1908–1910 (2007).
20. G. Toci, D. Alderighi, A. Pirri, and M. Vannini, "Lifetime measurements with the pinhole method in presence of radiation trapping: II—application to Yb^{3+} doped ceramics and crystals," Appl. Phys. B **106**(1), 73–79 (2012).
21. G. Toci, "Lifetime measurements with the pinhole method in presence of radiation trapping: I—theoretical model," Appl. Phys. B **106**(1), 63–71 (2012).
22. S. Chénais, F. Druon, F. Balembois, P. Georges, A. Brenier, and G. Boulon, "Diode-pumped Yb:GGG laser: comparison with Yb: YAG," Opt. Mater. **22**(2), 99–106 (2003).
23. R. Gaumé, B. Viana, D. Vivien, J. P. Roger, and D. Fournier, "A simple model for the prediction of thermal conductivity in pure and doped insulating crystals," Appl. Phys. Lett. **83**(7), 1355–1357 (2003).
24. K. Beil, S. T. Fredrich-Thornton, F. Tellkamp, R. Peters, C. Kränkel, K. Petermann, and G. Huber, "Thermal and laser properties of Yb:LuAG for kW thin disk lasers," Opt. Express **18**(20), 20712–20722 (2010).
25. Y. Guyot, H. Canibano, C. Goutaudier, A. Novoselov, A. Yoshikawa, T. Fukuda, and G. Boulon, "Yb^{3+}-doped $Gd_3Ga_5O_{12}$ garnet single crystals grown by the micro-pulling down technique for laser application. Part I: Spectroscopic properties and assignment of energy levels," Opt. Mater. **27**(11), 1658–1663 (2005).
26. Y. Guyot, H. Canibano, C. Goutaudier, A. Novoselov, A. Yoshikawa, T. Fukuda, and G. Boulon, "Yb^{3+}-doped $Gd_3Ga_5O_{12}$ garnet single crystals grown by the micro-pulling down technique for laser application. Part 2: Concentration quenching analysis and laser optimization," Opt. Mater. **28**(1-2), 1–8 (2006).
27. D. Alderighi, A. Pirri, G. Toci, and M. Vannini, "Tunability enhancement of Yb:YLF based laser," Opt. Express **18**(3), 2236–2241 (2010).

1. Introduction

Among crystal materials, garnets are the most widespread matrices used as laser host for rare earths dopants, due to a favorable combinations of parameters: ease of growing in large size, broad transparency range, good thermomechanical properties, compatibility with several trivalent ions as lasing dopants, such as Nd, Yb, Er, Ho, Tm, Pr. So far, several garnets have been proposed, YAG, LuAG and GGG being the most diffused.

Recently, the so-called mixed garnets, *i.e.* solid solutions of garnets with different compositions, have been proposed because the internal disordered structure may induce an inhomogeneous broadening on the absorption and emission spectra of the lasing ion. This feature is advantageous in particular for the generation and the amplification of ultrashort laser pulses. Several compositions, suitable for Yb^{3+} doping, are reported in literature. Partial substitution of the trivalent ion was used in $(Lu_xY_{1-x})_3Al_5O_{12}$ *i.e.* LuYAG (both crystals [1] and ceramics [2,3]), in ceramic $(Gd_xY_{1-x})_3Al_5O_{12}$ (GdYAG [4]) and in crystalline $(Lu_xGa_{1-x})_3Al_5O_{12}$ (LGGG) [5]. Partial substitution of the divalent ion was used in ceramic $(Y_3ScAl_4O_{12})$ [6]. Both the divalent and the trivalent ions were partially substituted in ceramic $\{YGd_2\}[Sc_2](Al_2Ga)O_{12}$ [7].

$Gd_3(Al_xGa_{1-x})_5O_{12}$ doped with Ce^{3+}, (GAGG:Ce^{3+}) [8,9] was initially proposed as a scintillator. Spectroscopic studies on Yb-Ho and Yb-Er doped GAGG were recently reported [10,11], as well as CW [12] and mode locked [13] lasing of Nd:GAGG with various Al/Ga

Optical Materials EXPRESS

ratios. Concerning Yb:GAGG, CW [14] mode-locked [15] and Q-switched [16] laser emission were demonstrated only for the ratio Al/Ga = 0.1/0.9 ($Gd_3(Al_{0.1},Ga_{0.9})_5O_{12}$) with 6.2% Yb doping. These previous investigations indicate that GAGG can be a very interesting laser host for Yb: the disordered structure induces a significant broadening of the emission band [14], but at the same time it does not degrade dramatically the thermal conductivity in comparison with other pure garnets (see for instance [17]).

These reasons motivated the interest for the study on other GAGG formulations with higher Al/Ga ratio, *i.e.* Al/Ga = 0.5/0.5, to assess the impact of this parameter on the Yb spectroscopic properties. Moreover, due to the significantly reduced content of highly volatile gallium oxide in Yb:$Gd_3(Al_{0.5},Ga_{0.5})_5O_{12}$ with respect to Yb:$Gd_3(Al_{0.1},Ga_{0.9})_5O_{12}$ it is expected that its composition is less affected by the loss of Ga_2O_3 during the growth. Finally, owing to marked difference of ionic radii of Ga and Al, the creation of antisites would be reduced, resulting in a crystal structure with low defects concentration. We present the first spectroscopic investigation and CW laser performance of a 2*at.*% Yb doped $Gd_3(Al_{0.5}Ga_{0.5})_5O_{12}$ crystal finding a maximum output power of 4.0 W, with a corresponding slope efficiency of 60%. Finally, we explored the tuning range, which resulted to be 54 nm, *i.e.* from 996 nm to 1050 nm.

2. Sample growth and properties

The sample was grown by the Czochralski method using a Malvern MSR4 puller with an automatic diameter control based on weighting the crucible. Starting materials (Gd_2O_3 (4N), Al_2O_3 (4N5) and Ga_2O_3 (5N)) were dried at 1000° C for 4 hours before weighting. Powders in appropriate molar ratios were mixed to obtain desired stoichiometry. Suitable amount of Yb_2O_3 (4N purity) was introduced in place of Gd_2O_3. Powders were pressed into a cylindrical pellet at 200 kPa and calcined at 1350° C for 6 hours before melting in a crucible. Single crystal was grown under N_2 atmosphere on <111> oriented seed (pulling rate of 2.5 mm/h, speed of rotation 20 rpm). Transparent crystal with 20 mm diameter and 50 mm in length was grown with a convex crystal melt interface from inductively heated iridium crucible of 40 mm in diameter, see Fig. 1. The doping level of Yb^{3+} was 2 *at.*% ($2.54x10^{20}$ ions/cm^3).

Fig. 1. Photograph of the as-grown crystal.

Phase analysis and structural refinement were performed on the powdered sample with a Siemens D5000 diffractometer (Ni-filtered Cu Kα radiation). Data were collected in the range 20°-100° (step of 0.02°, averaging time 10 s/step). The powder diffraction patterns were analyzed by the Rietveld refinement method using DBWS-9807 program [18] in order to determine the lattice constants. Rocking curve and 2Θ scan (Fig. 2) were recorded using the same diffractometer on (100) oriented single crystalline plates (step of 0.01°, averaging time 10 s/step). From these measurements the lattice constant resulted in a = 12.231 Å, as it is shown in Fig. 3.

Optical Materials EXPRESS

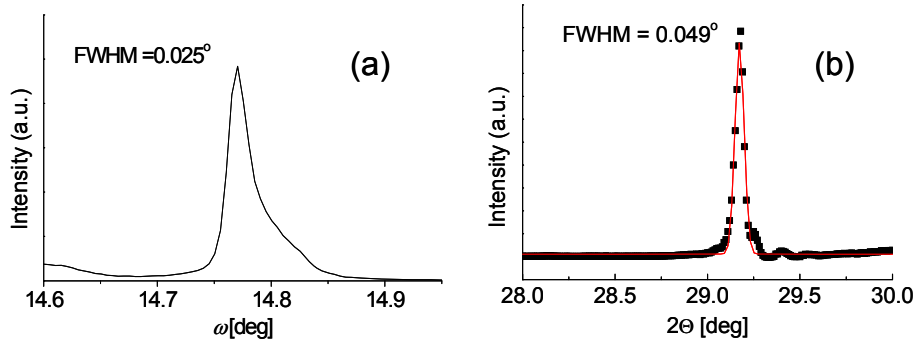

Fig. 2. X-ray rocking curve for the (400) reflection recorded for the crystal sample (a) and 2Θ scan curve. Black squares: experimental data; red line: Gaussian fit (b).

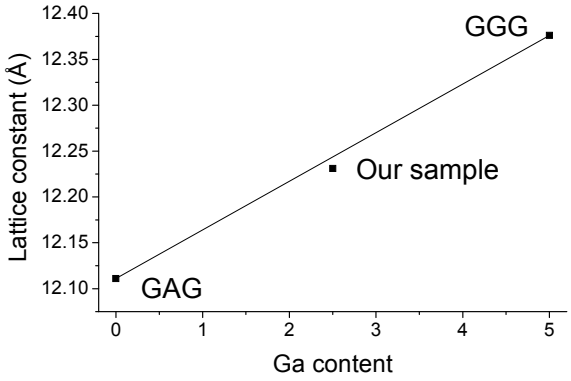

Fig. 3. Lattice constant as a function of the Ga content for GAG, GGG (data from JCPDS Card No. 13-0493 and No. 32-0383 respectively) and from our sample. The solid line is the linear interpolation between GAG and GGG.

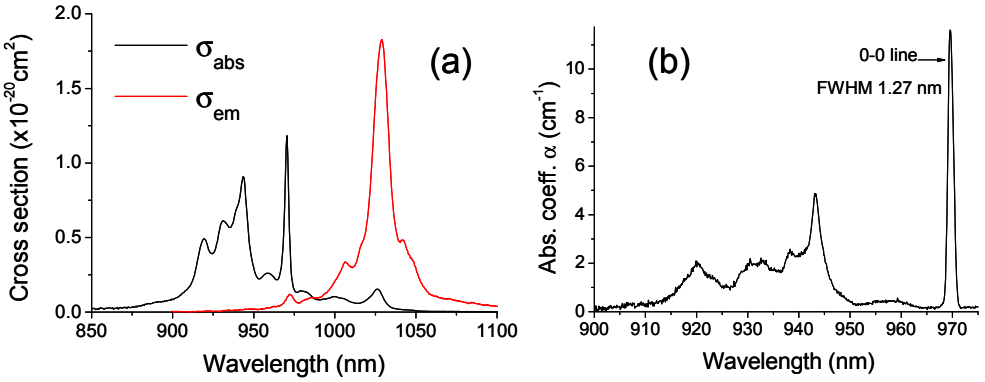

Fig. 4. Absorption and emission cross section spectra of the Yb^{3+} $^2F_{7/2}$-$^2F_{5/2}$ transition at room temperature (a) and absorption spectrum at 5 K (b).

Figure 4(a) reports the absorption cross section spectrum (σ_{abs}) measured with a Varian Cary 5E spectrophotometer (bandwidth 0.5 nm). The absorption spectrum features a broad band between 905 nm and 945 nm, peaked at 943 nm (peak $\sigma_{abs} = 0.91 \times 10^{-20}$cm^2), well suited for pumping with semiconductor lasers. The zero-phonon line is located at 970.3 nm,

Optical Materials EXPRESS

with a peak value of σ_{abs} of 1.18×10^{-20}cm^2. The absorption cross section here is higher, but the relatively narrow width of the absorption peak (about 3.4 nm FWHM) requires a tighter wavelength control of the pump source.

The absorption spectrum recorded at 5 K (Fig. 4(b)) shows that the zero phonon absorption line has a single peak structure, with a FWHM of 1.27 nm.

The lifetime of the Yb^{3+} level $^2F_{5/2}$ was measured with two independent methods, both aimed to minimize radiation trapping effects: on a finely powdered sample (obtained by mechanical crushing of a bulk sample) and on a bulk sample by means of the so-called pinhole method [19] using the experimental set-up described in [20]. As it is known [19-21], the reabsorption of the emitted fluorescence lengthens the fluorescence lifetime with respect to the upper level lifetime. Both measurements techniques resulted in the same value, 0.91 msec. For comparison, the fluorescence lifetime on a bulk sample without pinhole resulted in 1.1 ms, with only about 20% increase owing to the low doping level of the sample.

Luminescence spectrum was acquired by Dongwoo Optron DM711 monochromator having a focal length of 700 mm, coupled with an InGaAs detector. The measurement was carried out on a finely powdered sample, so as to avoid reabsorption effects: due to the small size of the powder grains, the emitted photon has a low probability to be reabsorbed before to leave the grain volume. The emission cross section spectrum was obtained from the luminescence spectrum using the Füchtbauer-Ladenburg formula. The emission cross section spectrum (σ_{em}, see Fig. 4) has a peak value of 1.83×10^{-20}cm^2 at 1027.0 nm, with a FWHM of 12.1 nm.

Thermal conductivity was measured by the steady-state longitudinal heat-flow method. The crystal, in the form of rod 10 mm long and 3x3 mm^2 of cross section, was mounted in a temperature controlled liquid He cryostat. The temperature drop along the sample did not exceed 0.2 K; extreme care was taken to eliminate parasitic heat flow between the sample and its surrounding. The thermal conductivity at room temperature is 8.1 ± 0.6 W/(m K). This value is slightly higher than Yb:GGG (8 W/(m K) undoped, 7.5 W/(m K) with 5.7% doping) [22], similar to Yb:YAG (about 8 W/(m K) with 2% doping) [23] and slightly lower than undoped LuAG (reported between 8.3 and 9.6 W/(m K)) [24]. The overall error on the thermal conductivity results from the statistical error (which did not exceed 2%) and from the systematic error (estimated to be 6%, due to the inaccuracy in the measurement of the distance between the thermometers providing the temperature gradients). It must be also noticed that this value is consistent with the value (7.8 W/(m K)) measured by Kuwano *et al.* [17] for 1% Nd doped $Gd_3(Al_{0.4},Ga_{0.6})_5O_{12}$, *i.e.* with a host composition close to the one analyzed here.

3. Laser emission measurements

The sample was shaped as a parallelepiped with 4 × 4 × 10 mm^3 sides. It was inserted with one of the 4 mm sides parallel to the axis of the end-pumped laser cavity shown in Fig. 5. Mirrors EM and FM are dichroic (high transmission for the pump wavelength, high reflection for the laser wavelength), set at a distance of 55 mm. The distance between FM and the output coupler OC is 165 mm. The sample is soldered with Indium by its end face on a copper heat sink cooled by water at 18°C, and placed near to the EM. As the sample has no AR coating, to reduce the Fresnel losses it was oriented to re-inject the face reflections on the cavity axis. The pump source is a fiber coupled laser diode (wavelength 938 nm, 200 μm fibre core diameter, 0.22 fibre NA). The fiber tip is reimaged on the sample by two achromatic doublets (nominal magnification 1). The pump intensity distribution in the focal plane is almost Gaussian (radius ~150 μm @ $1/e^2$). The maximum incident power was 22 W CW. The pump absorption was measured during the laser action at each incident power, by measuring the residual power transmitted by the sample, refocused by a collecting lens (L) on the auxiliary power meter M. Tunable emission was obtained by placing a Brewster ZnSe prism

Optical Materials EXPRESS

(apex angle 41.8°) and a slit placed between FM and OC. The wavelength was measured with a 60 cm focal length spectrometer equipped with a multichannel detector (resolution 0.4 nm).

Figure 6 reports the laser output power as a function of the absorbed pump power obtained with several OCs, having a transmission spanning from 2.2% to 57.6%.

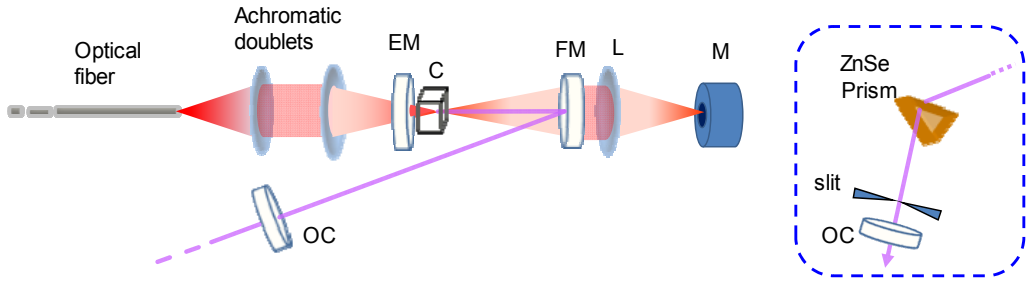

Fig. 5. Laser cavity. EM: end mirror (flat); FM: folding mirror (spherical, radius of curvature 100 mm); OC: output coupler (flat); C denotes the lasing material. M: auxiliary power meter. The inset on the right shows the arrangement for the tunable cavity.

The results in terms of laser output power, slope efficiency, optical-to-optical efficiency and radiation wavelengths are summarized in Table 1. The sample absorbed about 44% of the incident pump power (up to 9 W).

Lasing occurred on a single peak (typical linewidth 1.4 nm FWHM). The wavelength shifted from 1030 nm to 1026 nm for increasing T. With T = 2.2% emission occurred at 1043.9 nm for output power below 0.72 W; above this level the laser emitted simultaneously at 1043.9 and 1030 nm.

The tuning range was investigated by the tunable cavity described above, using the OC with T = 2.2%. In these measurements, the crystal was pumped in quasi-CW regime (20 ms duration, frequency 10 Hz). The peak output power as a function of the emission wavelength is shown in Fig. 6(b). The maximum output power (300 mW) is obtained at 1026 nm while the tuning curve extends from about 996 nm to 1050 nm.

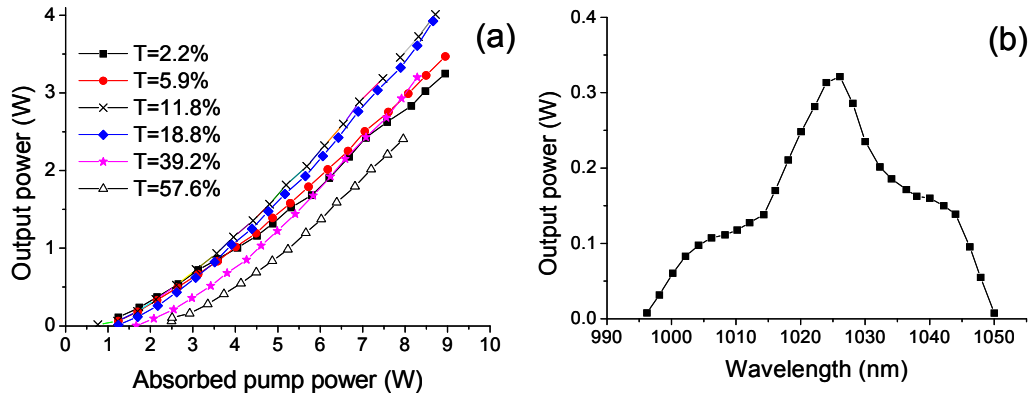

Fig. 6. Output power vs. absorbed pump power obtained with several OCs with different transmission T (a). Output power vs. wavelength obtained with the tunable cavity (b).

Optical Materials EXPRESS

Table 1. Emission parameters for several OC transmission T. λ: wavelength; P_{max}: max. output power; η_S, η_O: slope and optical-to-optical conversion efficiency.

T (%)	λ (nm)	P_{max} (W)	η_S (%)	η_O (%)		T (%)	λ (nm)	P_{max} (W)	η_S (%)	η_O (%)
2.2	1043.9 1030.0	3.25	45.6	35.7		18.8	1026.6	3.93	58.6	43.5
5.9	1030.0	3.47	49.2	38.0		39.2	1026.4	3.20	54.3	38.0
11.8	1026.8	4.01	60.8	46.0		57.6	1026.0	2.41	46.2	29.0

4. Discussion

The assessment of the crystal structure by means of X-ray diffraction (Fig. 2) resulted in a crystal lattice constant a = 12.231 Å. This value is very close to the average value (12.2435 Å) between the lattice constant of $Gd_3Ga_5O_{12}$ (GGG, JCPDS Card No. 13-0493, a = 12.376 Å) and $Gd_3Ga_5O_{12}$ (GAG, JCPDS Card No. 32-0383, a = 12.111 Å), see Fig. 3. This implies that the actual composition of our sample is very close to the nominal one, *i.e.* $Gd_3(Al_{0.5}Ga_{0.5})_5O_{12}$.

Concerning the zero-phonon line (Fig. 3) we notice that in the low temperature spectrum it appears as a single peak at 969.6 nm. This indicates that the Yb ions are located on a single crystallographic site: multiple sites, originated for instance by lattice defects, would result in a splitting of the zero-phonon line. The disordered crystal structure results in an inhomogeneous broadening of the zero phonon line of 1.27 nm. At room temperature, due to the mixed composition the zero-phonon line shifts from 971 nm (observed in GGG [25]) to 970.3 nm in our GAGG while the peak absorption increases from 0.7×10^{-20} cm^2 in GGG to 1.18×10^{-20} cm^2 in our sample. An increase from 0.45 to 0.91 ($\times 10^{-20}$ cm^2) of the peak absorption, which is located near 943 nm, is observed as well. For the GAGG composition with Al/Ga = 0.1/0.9 [14] the absorption cross section was more similar to GGG (0.56×10^{-20} cm^2 @ 942 nm and 0.43×10^{-20} cm^2 on the zero line). The emission spectrum is peaked at 1027 nm, shifted by 2 nm from the peak position in Yb:GGG (at 1025 nm). The peak emission cross section is similar to other garnets (1.83×10^{-20} cm^2 vs. 2.0×10^{-20} cm^2 in GGG, 2.3×10^{-20}cm^2 in YAG, 2.5×10^{-20}cm^2 in LuAG [24]), but the peak is broader (12.1 nm FWHM) than in GGG, YAG and LuAG (8 nm, 9 nm and 7.3 nm respectively). It must be noticed that the emission bandwidth of the Yb:GAGG with Al/Ga = 0.1/0.9 reported in [14] is slightly broader (13.8 nm) than in our composition.

The lifetime of the $^2F_{5/2}$ level (0.91 ms) was longer than in GGG (0.83 ms [26]) and similar to Yb:YAG (0.95 ms [19]) and LuAG (0.965 msec [24]). For the lifetime we obtained this same value from two independent methods (that is, on powdered samples and by means of the pinhole method, as described above), both aimed to minimize reabsorption effects. This result should then have a high degree of reliability.

It must be noticed that Zhang *et al.* [14] reported a higher value (1.38 ms) of the $^2F_{5/2}$ level lifetime. This value is much longer than our findings; due to their low Al/Ga ratio (0.1/0.9), a value more similar to Yb:GGG (0.83 ms, see [26]) could be expected. On the other hand, the measurement reported in that paper is simply defined as "fluorescence decay measurement", and no remedies are reported to avoid reabsorption effects. Therefore, this result may be affected by radiation trapping effects. As this value is needed for the evaluation of the emission cross section spectrum (with the Fuchtbauer-Ladenburg formula), this could also lead to an underestimation of the emission cross section (with a peak value, 1.1×10^{-20}cm^2, which is indeed much lower than in Yb:GGG). For these reasons in our opinion the studies on Yb:GAG crystals are available in literature, nor even results regarding the laser emission.

Regarding the laser emission, the sample has shown a maximum output power of 4.0 W CW with high slope and optical efficiencies (respectively 60% and 46% in the most favorable conditions), *i.e.* higher than those reported so far for Yb:GAGG with Al/Ga = 0.1/0.9 (respectively 53.2% and 41.6% [14]), even though with a lower maximum output power.

Optical Materials EXPRESS

Recently, Zhao *et al.* [16] reported the high repetition rate pulsed operation of a 6% doped Yb:GAGG with Al/Ga = 0.1/0.9, obtained with an actively Q-switched cavity, with a maximum average output power of 1.4W and a maximum slope efficiency of 32%. These values are quite lower than our results, but it must be taken into account that usually the Q-switch devices introduce additional intracavity losses which reduces the energy extraction efficiency with respect to the simple CW operation. The spectroscopic data reported there are recalled from [14].

Our slope efficiency is also higher than that previously reported for Yb:GGG (46% [22]). In our case the output power was limited only by the available pump power, but we did not observe signs of output degradation due to thermal effects.

The tuning range was quite broad, from 996 nm to 1050 nm (54 nm). The peak power occurs at 1026 nm, slightly shorter than the peak of the emission cross section spectrum (1027 nm) and similar to the free running lasing wavelength obtained with high output losses. To our knowledge this is the first assessment of the tuning range for Yb:GAGG of any composition. A comparison with previous results is possible only with Yb:GGG: the tuning curve reported in [22] was peaked at 1038 nm and extended from 1022 nm to 1075 nm, *i.e.* with a similar width, but shifted to longer wavelengths.

To support this result we calculated the theoretical tuning range achievable with our experimental set-up in conjunction with the emission bandwidth of our sample. For this purpose, we used a previously reported model [27] based on rate equations. The small signal gain is calculated as a function of the wavelength, using the absorption and the emission cross section spectra of the sample and the parameters of the experimental set up (pump beam size and power, cavity mode size, cavity roundtrip losses). The tuning range is the wavelength interval where the small signal gain matches or exceeds the cavity losses over a roundtrip. In our experiment, the roundtrip losses of the tunable cavity were evaluated at about 18% (due to the relatively high Fresnel losses introduced by the ZnSe prism). The calculated tuning range extended from 1003 nm to 1053 nm. This result is fairly in agreement with the experimental results. It must be noticed anyway that this kind of calculations is very sensitive to the uncertainties in the determination of the emission cross section spectrum, in particular on the twings of the emission peak, and it cannot replace an experimental evaluation.

5. Conclusions

We have presented the spectroscopic investigation and laser emission demonstration of Yb:GAGG with 0.5/0.5 Al/Ga balance. To our knowledge, this is the first characterization of the spectroscopic and laser properties of Yb:GAGG with such a high Al/Ga ratio. This crystal has demonstrated to be an interesting laser material for high power laser applications, with good potentialities for the generation and the amplification of ultrashort laser pulses.

The main effect of the mixed composition on the Yb spectroscopy is a significant broadening (about 50% FWHM) and a slight shift (about 2 nm) of the emission spectrum with respect to the parent composition Yb:GGG. This broad bandwidth should allow the generation and amplification of ultrashort laser pulses in the sub-100 fs time scale. The upper laser level lifetime is longer than in Yb:GGG, which is beneficial in terms of energy storage capabilities. The thermal conductivity at room temperature is quite high, similar to YAG and LuAG with similar doping levels, which is favorable for the development of high power laser systems. Such a high thermal conductivity was already reported in literature (see for instance [17]), nonetheless it is quite unusual in the scenario of the disordered crystals.

In terms of laser performance, the material has shown a quite high slope efficiency (up to 60%), slightly higher than that reported so far for Yb:GGG [22] and for Yb:GAGG with ratio Al/Ga = 0.1/0.9 [14]. We point out that in our experiment the pumping conditions were under-optimized, due to the low doping of the sample (resulting in a relatively low pump absorption) which in turn required a long sample length (4 mm), resulting in relatively poor matching between the highly divergent pump beam and the laser mode.

Optical Materials EXPRESS

The tuning range was blue-shifted with respect of Yb:GGG and only slightly broader, despite that the emission spectrum is substantially broader than in Yb:GGG. This is probably due again to the relatively low pump absorption of the sample that prevents laser oscillation above 1055 nm, where laser threshold increases due to the decreasing emission cross section. Improvements are expected in terms of slope efficiency and tuning range by using samples with a higher doping and a smaller thickness.